UNCOVERING FRICTION-DOMINANT STRUCTURES IN TURBULENCE VIA DNS AND EXPLAINABLE AI

Sergio Hoyas
IUMPA,
Universitat Politècnica de València
Camino de vera, Valencia 46022, Spain
serhocal@mot.upv.es

Andrés Cremades
IUMPA,
Universitat Politècnica de València
Camino de vera, Valencia 46022, Spain
ancrebo@upv.es

Federica Tonti
Department of Aerospace Engineering,
University of Michigan,
Ann Arbor, MI 48109, United States
ftonti@umich.edu

Ricardo Vinuesa
Department of Aerospace Engineering,
University of Michigan,
Ann Arbor, MI 48109, United States
rvinuesa@umich.edu

ABSTRACT

This work introduces a new definition of coherent structures in turbulent channel flow, derived from their relevance to wall-shear stress and energy dissipation, based on Direct Numerical Simulations (DNS) and explainable deep learning (XDL). The structures are compared to the definition of traditional structures and the high-importance structures for the evolution of the flow. These newly identified regions are shown to dominate frictional processes, surpassing the role traditionally attributed to classical structures. Importantly, their characteristic size falls within a narrow range, facilitating their systematic identification and targeting. This approach opens the door to the design of advanced algorithms and devices that directly control such structures, thereby enabling more efficient drag-reduction strategies.

Introduction

Turbulence remains an unsolved problem with profound implications for everyday life. A promising new approach to understanding turbulence is explainable deep learning (XDL) (Cremades *et al.*, 2025*a*). Explainable deep learning provides the tools to quantify importance using an objective definition, and is the methodology applied in the present analysis (Lundberg & Lee, 2017). Among the many facets of turbulence, energy dissipation is the most critical in the context of the climate crisis, as it is the primary mechanism by which energy is lost in fluid flows. When turbulent flows interact with solid boundaries, this dissipation appears as drag or friction. Such losses are commonly quantified using the skin-friction coefficient c_f, which is introduced later. Remarkably, up to 15% of global energy consumption is wasted as turbulent drag within the first millimeter of boundary layers in moving vehicles or in pipeline flows (Jiménez, 2018).

Efforts to study and mitigate frictional losses date back to the pioneering experiments of Hagen and Poiseuille in the 19th century. From an engineering perspective, Moody's diagram has long been a cornerstone for practical applications (Moody, 2022). More recently, computational fluid dynamics (CFD) has become a standard tool to optimize vehicle and pipeline design (Slotnick *et al.*, 2014). Yet, these models remain intrinsically limited (Pope, 2000), motivating the search for alternative approaches to drag reduction. One promising avenue lies in unraveling the nonlinear dynamics of turbulent structures and their role in transporting momentum and energy from the wall to the outer flow (Jiménez, 2018).

In this context, Guastoni *et al.* (2021) showed that deep reinforcement learning can identify remarkably efficient strategies for drag reduction, which substantially modify the size and geometry of near-wall turbulent structures. Yet, these control schemes largely operate as black boxes, leaving open the fundamental question of which mechanisms underpin their effectiveness. More recently, Cremades *et al.* (2024) examined the role of a particular class of structures, the so-called Q-events, in dictating the dynamics of wall turbulence. Their analysis revisited and unified three decades of prior knowledge, leading to a clearer identification of the structures most strongly linked to wall friction. Building upon this framework, the present study evaluates the relative contribution of several canonical coherent structures to the prediction of wall-shear stress and, consequently, to the associated energy dissipation.

While the focus in Cremades *et al.* (2024) was on coherent structures, and their effect on friction was later examined in Hoyas *et al.* (2025), the authors took a further step. Instead of evaluating the relevance of predefined structures, they investigated the importance of each point, thereby allowing the definition of coherent structures, named SHAP structures, (Cremades *et al.*, 2025*b*). These structures implicitly capture causal effects in the flow and could be used by Beneitez *et al.* (2025) to control and reduce the wall friction in turbulent flows actively.

The previous ideas suggest that assessing structures that target the friction coefficient rather than the flow evolution might improve control algorithms. In the present work, we focus on assessing the contribution of each point to the skin-friction coefficient, quantified by $\partial_y \overline{U}$, comparing the physics of the structures to the velocity-based SHAP structures and the traditional coherent structures.

Methods

The methodology employed in this work can be divided into three main stages. First, a surrogate model was developed using a U-net (Ronneberger *et al.*, 2015) deep-learning architecture, trained on a database of 10,000 instantaneous flow fields. This U-net uses a similar architecture to the network employed in Cremades *et al.* (2025*b*), with the peculiarity that in the specific application presented in this work, the network predicts bi-dimensional data, the friction coefficient over the wall, from three-dimensional data, the velocity field. The architecture requires a dimensional compression along the wall-normal direction. This compression is produced by a set of three-dimensional convolutions followed by an average pooling with kernels of shape $(1,k,1)$, so they do not affect the wall-parallel directions. Training continued until the relative error of the predictions fell below approximately 1% of the maximum value across the database, ensuring the model's accuracy.

Second, the trained model was used to compute the importance of each input grid point for predicting the friction coefficient, employing the gradient-SHAP algorithm. For this purpose, the model was modified to produce a single output representing the mean squared error of the reconstruction of the friction coefficient along the wall.

Finally, once the SHAP values were obtained, they were used to define the high-importance regions (hereafter referred to as SHAP structures), which were then analyzed to evaluate their physical properties. For the definition of the friction SHAP structures, the expression of Cremades *et al.* (2025*b*) has been used for the reason of consistency with the previous analysis:

$$\sqrt{\phi_u^2(x,y,z,t)+\phi_v^2(x,y,z,t)+\phi_w^2(x,y,z,t)} > H\sqrt{(\phi_u')^2(y)+(\phi_v')^2(y)+(\phi_w')^2(y)}, \tag{1}$$

In this expression, the instantaneous value of the SHAP values ϕ_u, ϕ_v, and ϕ_w is compared against their expected intensity value ϕ_u'.

Using the gradient-SHAP methodology (Erion *et al.*, 2021), we compute an importance score for each grid point in a turbulent channel flow with a friction Reynolds number $Re_\tau = u_\tau h/\nu = 125$. The gradient-SHAP methodology evaluates the sensitivity of the U-net with respect to each input feature (the velocity components at each grid point) integrated from a reference or non-informative flow field to the actual flow field. The gradient-SHAP algorithm calculates the importance of the grid points using the expression:

$$\phi_{\mathrm{i}}(x_{\mathrm{in}}) = \mathbb{E}_{x_{\mathrm{ref}},\alpha\sim U(0,1)}\left[\left(x_{\mathrm{in}_i}-x_{\mathrm{ref_i}}\right)\frac{\partial F\left(x_{\mathrm{ref}}+\alpha\left(x_{\mathrm{in}}-x_{\mathrm{ref}}\right)\right)}{\partial x_{\mathrm{in}_i}}\right], \tag{2}$$

where the importance of the feature i, $\phi_{\mathrm{i}}(x_{\mathrm{in}})$ is calculated as the expectation of the value of the gradient over the sample of n interpolated fields from the reference, x_{ref}, to the input, x_{in}, $\alpha \sim U(0,1)$.

These SHAP values highlight the most influential points for the causal relationships captured by the deep-learning model. The physical interpretation of SHAP values depends on the model's output. The original analysis of Cremades *et al.* (2025*b*) focused on structures that condition the flow, whereas in this case the model evaluates the friction coefficient; thus, the SHAP values reveal the flow regions that play the largest role in the evolution of near-wall shear.

The importance scores measure the influence of each grid point on the prediction of the wall-shear stress over a time horizon $\Delta t^+ = \Delta t, u_\tau^2/\nu = 5$, where h is the channel half-height, ν the fluid kinematic viscosity, $u_\tau = \sqrt{\tau_{\mathrm{w}}/\rho}$ the friction velocity (with τ_{w} the wall-shear stress and ρ the fluid density), and Δt the time interval between snapshots (Pope, 2000).

Applying the gradient-SHAP methodology yields a vector field of importance values, denoted as ϕ, which quantify the causal contribution of each grid point to the flow evolution or to the friction coefficient c_f, defined as:

$$c_f = \frac{2\nu}{U_b^2}\frac{\mathrm{d}U}{\mathrm{d}y}, \tag{3}$$

where the wall-normal rate of change of the streamwise velocity $\mathrm{d}U/\mathrm{d}y$ is proportional to the skin-friction coefficient, and U_b is the bulk velocity.

These SHAP values provide a measure of how strongly individual regions influence the dynamics. These regions have a causal nature, as demonstrated in the supplementary material of Cremades *et al.* (2025*b*), and thus are the most influential in the evolution of the flow. Therefore, as outlined earlier, the model's formulation ensures that the SHAP values highlight the most relevant grid points for the evolution of the friction, the desired physical mechanism, and consequently, to control this mechanism in the flow. For this reason, the analysis of the friction-based SHAP structures is crucial for the development of future active control technologies for drag reduction.

Results

In Hoyas *et al.* (2025) we extended the methodology and database of Cremades *et al.* (2024), identifying the most informative traditional coherent structures for predicting frictional losses in the turbulent channel flow. These traditional coherent structures are visualized in Figure 1, where the Q-events (sweeps and ejections) are shown in the left panel and the streaks and vortices in the right panel. To quantify the importance of the traditional structures, two types of SHAP values were employed. The first SHAP definition is associated with the reconstruction of the velocity-fluctuation field, $|\phi^{\mathbf{u}}|$, and the second structure is linked to the skin-friction coefficient, $|\phi^{c_f}|$. The results showed that the coherent structures most important for predicting the flow evolution differ from those most relevant for predicting the evolution of friction at the wall. In this work, the ejection-like structures are shown to contain more information about the evolution of velocity. These structures include ejections and low-velocity streaks. The former have high importance values for both flow evolution and friction prediction, while the latter are mostly important for flow evolution. This idea shows that friction is mostly associated with Q-events. Although streaks are crucial for understanding the evolution of the turbulent field, they are not strongly linked to friction. Concerning friction, the phenomenon is closely related to enstrophy. Consequently, the sweeps, which are the structures transporting the information towards the wall, are the most relevant for the friction coefficient, Figure 2. Similar conclusions are drawn when the importance is divided by the structure's total volume. In this case, the stronger influence of sweeps compared to the other structures on predicting the friction coefficient is more pronounced, as sweeps are smaller than ejections in this flow regime. Note that for the specific importance, the high-velocity streaks (sweep-like structures) gain

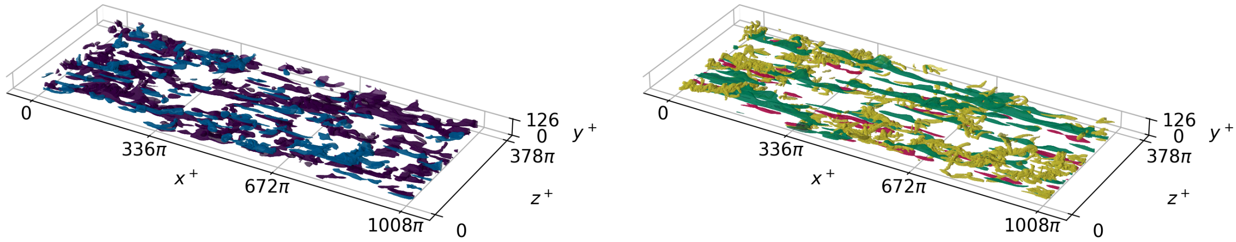

Figure 1. Instantaneous visualization of the different types of coherent structures at the same time, but separated in two panels to facilitate their visualization. Ejections (purple), sweeps (blue), low-velocity streaks (green), high-velocity streaks (pink), and vortices (yellow).

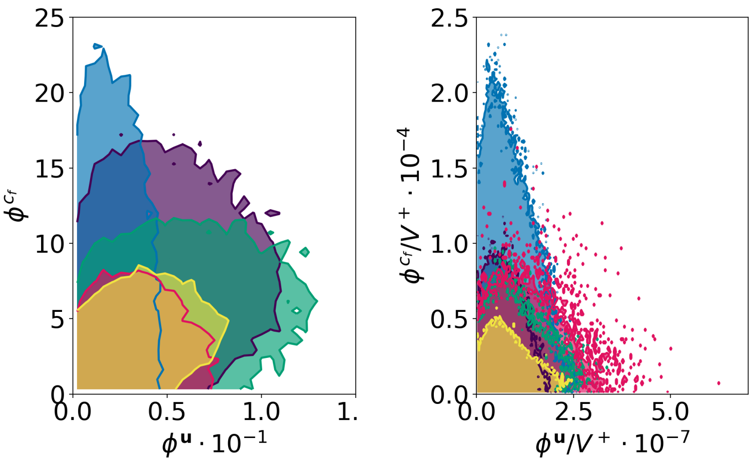

Figure 2. JPDF of the SHAP values $|\phi^{\mathbf{u}}|$ and $|\phi^{c_f}|$ (left), and divided by volume (right). Ejections (purple), sweeps (blue), low-velocity streaks (green), high-velocity streaks (pink), and vortices (yellow).

importance relative to the ejections, proving that those regions with high velocity are the most influential for the friction.

To improve flow control and reduce drag, the key structures that generate friction need to be targeted. The local SHAP values for predicting the future friction are calculated and compared to the SHAP values for predicting the flow evolution. The main difference between the two approaches is observed in the wall-normal distribution of the SHAP values (Figure 3). While the intensity of the SHAP values for predicting the flow evolution is concentrated in a range of wall-normal distances between 5 and 60 wall units and are distributed across all velocity components. For the friction coefficient, importance lies below the streaks and in the streamwise component of the velocity. The friction-based SHAP shows a peak between 3 and 5 wall units, below the range where the velocity-based SHAP is strong. Note that in the friction coefficient case, the relevance of the structures decays above the streaks, $y^+ > 20$, where the SHAP value is negligible compared to the peak in the inner region. The coherent structures are calculated by detecting regions of high intensity relative to the expected intensity at their wall-normal locations, as in equation (1). The instantaneous visualization of the percolated SHAP structures for both definitions is provided in Figure 4.

The distribution of the velocity inside both definitions of SHAP structures along the wall normal velocity is presented in Figure 5. The velocity-based SHAP structures present two regions of high density of structures: the first corresponds to high-velocity or sweep-like regions located from the wall to the streaks ($y^+ \approx 15$); the second, on the other hand, is composed of low-velocity or ejection-like regions from the streaks to the center of the channel. This density function shows that the SHAP values mostly highlight the low-velocity regions ($y^+ < 15$), where high-velocity structures or sweep-like structures penetrate, and the high-velocity regions ($y^+ > 15$), where the low-velocity structures enter. However, for the friction coefficient, a different picture emerges. In this case, the sweep-like regions near the wall are the most highlighted structures, demonstrating that, for friction, the most relevant structures are the high-velocity regions that transport energy to the wall. Note that the density functions for the friction coefficient present more oscillations due to the decay in the SHAP value produced above the streaks and the low SHAP intensity far from the wall. This result is consistent with Hoyas *et al.* (2025), where the sweeps clearly concentrated importance for the prediction of wall friction, and with Osawa & Jiménez (2024), who reported that the high-velocity regions were the ones transporting more information in turbulent flows.

Finally, the instantaneous coincidence of the SHAP structures with the classical coherent structures is shown in Figure 6. The figure shows that the velocity-based SHAP structures exhibit constant overlap with Q-events along the wall-normal direction, with sweeps near the wall and ejections far from the wall. For a wall-normal distance of $y^+ \approx 15$, the velocity-based SHAP structures highlight the most important region of the streaks. Finally, these structures are not located in regions of high vorticity.

Concerning the friction-based structures, the coincidence is mostly detected near the wall, for $y^+ < 15$, where the SHAP

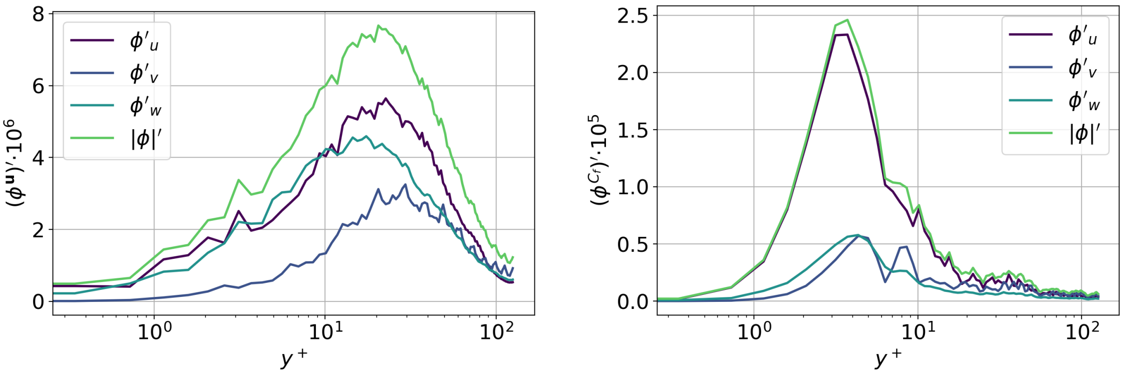

Figure 3. Intensity of the SHAP values as a function of the wall-normal velocity, velocity-based SHAP, $|\phi^{\mathbf{u}}|$ (left) and the friction coefficient-based SHAP, $|\phi^{c_f}|$ (right).

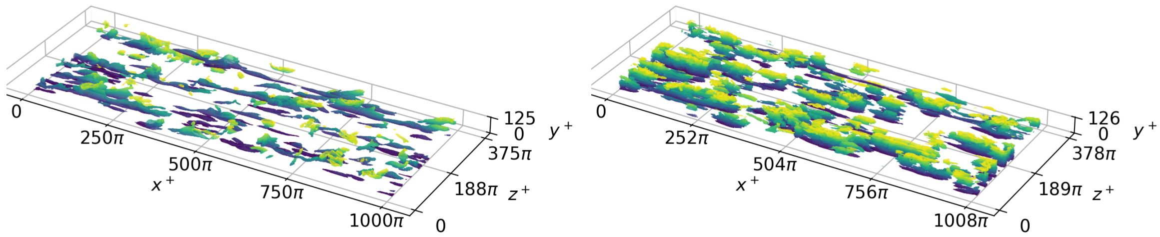

Figure 4. Visualization of SHAP structures based on the velocity, $|\phi^{\mathbf{u}}|$ (left) and the friction coefficient, $|\phi^{c_f}|$ (right).

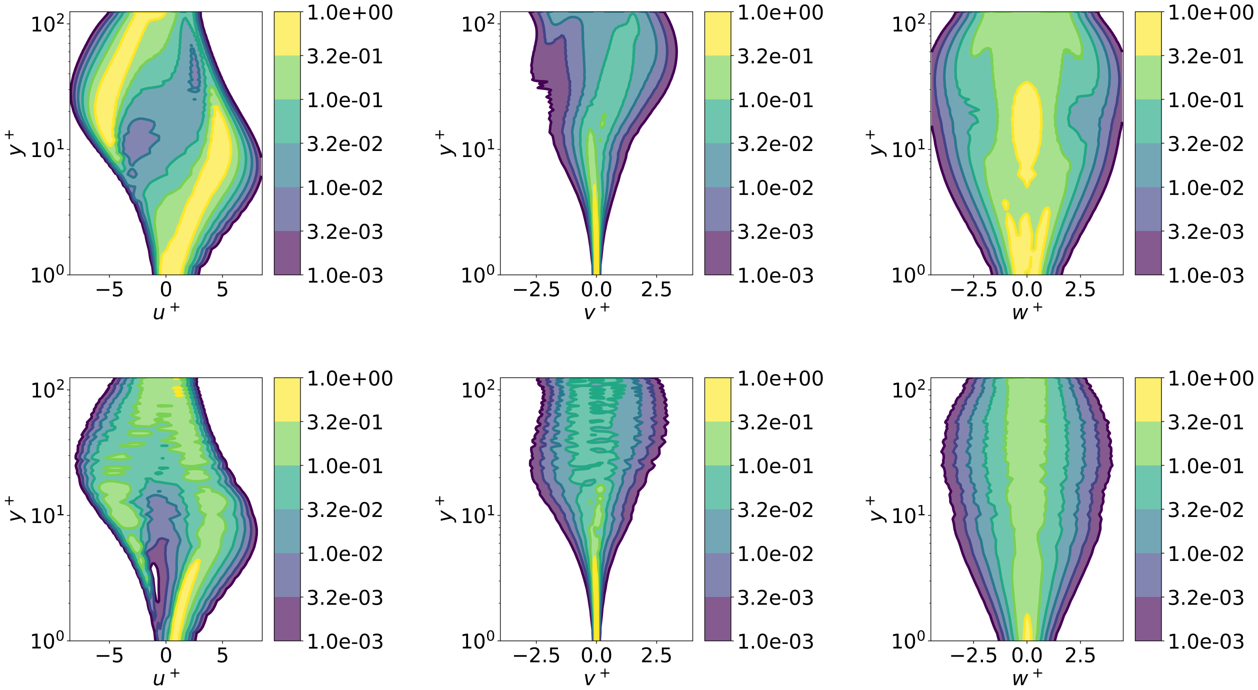

Figure 5. JPDF of the velocity and the wall normal position of the SHAP structures based on the velocity, $|\phi^{\mathbf{u}}|$ (top) and the friction coefficient, $|\phi^{c_f}|$ (bottom).

structures mostly overlap with the sweeps for $y^+ < 10$ and with streaks for $y^+ \approx 15$. For $y^+ < 10$, both SHAP definitions present similar levels of agreement with the sweeps; however, as the wall-normal distance is increased, the differences between the two definitions increase. The coincidence with the streaks of the friction-based structures is approximately half

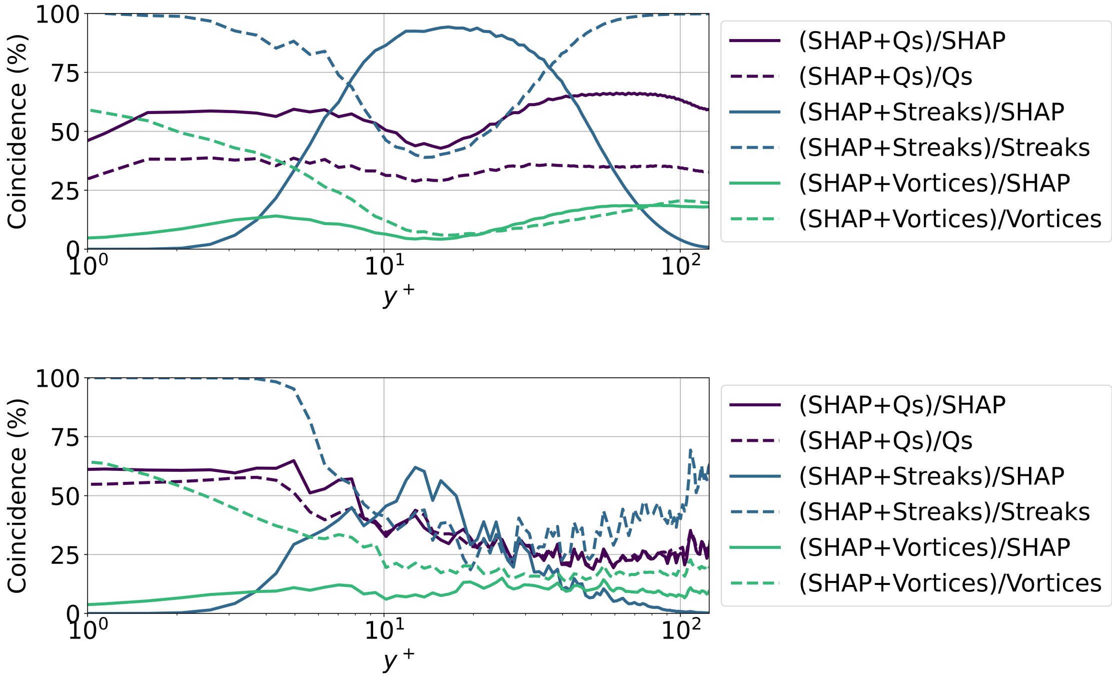

Figure 6. Instantaneous coincidence of the SHAP structures and the classical structures. Coincidence of the velocity-based SHAP structures (left) and friction-coefficient-based SHAP structures (right) with Q-events (purple), streaks (blue), and vortices (green).

that of the velocity-based structures, and at greater distances the SHAP values for the friction case are extremely low, while the velocity-based structures detect important flow patterns in these regions.

Conclusions

In this work, the most important structures for predicting the friction coefficient were identified by calculating SHAP values for each grid point. The methodology has been divided into three main stages: training a deep learning model to predict the future value of the friction coefficient, calculating the SHAP values for every grid point, and, finally, percolating the friction-based SHAP structures.

The results show that the high-intensity SHAP values for the friction coefficients are located below the wall-normal position of the streaks, in a narrow band between 3 and 5 wall units, where high-velocity events enter regions of low velocity and high shear. This idea opposes the conclusions presented for the velocity-based SHAP values (Cremades *et al.*, 2025*b*), where the peak of importance was located around the streaks extending from 5 to 30 wall units. The friction-based coherent structures are related to the wall-attached sweeps, which account for most of the system's importance, similarly to what was detected in the previous work of Hoyas *et al.* (2025). In contrast, the velocity-based structures match all Q-events (sweeps and ejections) and streaks.

The research presented here is part of an ongoing investigation aimed at identifying the key mechanisms that govern wall-bounded turbulence and friction, and is noted as the next step in the conclusions of (Hoyas *et al.*, 2025). Although the work is still in progress, all studies carried out so far indicate very encouraging trends, suggesting that the proposed methodology can identify the most influential regions for drag generation and control. These preliminary insights provide strong motivation to continue in this direction, as they open new opportunities for both fundamental understanding and practical applications. The complete set of results, including a detailed analysis of the identified structures and their implications for turbulence control, will be presented during the conference.

Acknowledgments

SH was funded by project PID2021-128676OB-I00 by MCIN/AEI/10.13039/501100011033 and by "ERDF A way of making Europe", by the European Union (SH).

Credit statement

Sergio Hoyas: Data curation, Writing – original draft, Writing – review & editing, Resources. **Andres Cremades**: Investigation, Formal analysis, Conceptualization, Writing – original draft, Writing – review & editing. **Federica Tonti**: Investigation, Formal analysis, Writing – review & editing. **Ricardo Vinuesa**: Conceptualization, Investigation, Writing – review & editing, Supervision, Funding adquisition.

REFERENCES

Beneitez, Miguel, Cremades, Andres, Guastoni, Luca & Vinuesa, Ricardo 2025 Improving turbulence control through explainable deep learning. *arXiv preprint arXiv:2504.02354* .

Cremades, Andrés, Hoyas, Sergio, Deshpande, Rahul, Quintero, Pedro, Lellep, Martin, Lee, Will Junghoon, Monty, Jason P, Hutchins, Nicholas, Linkmann, Moritz, Marusic, Ivan & Vinuesa, Ricardo 2024 Identifying regions of importance in wall-bounded turbulence through explainable deep learning. *Nature Communications* **15** (1), 3864.

Cremades, Andrés, Hoyas, Sergio & Vinuesa, Ricardo 2025*a* Additive-feature-attribution methods: A review on explainable artificial intelligence for fluid dynamics and heat transfer. *International Journal of Heat and Fluid Flow* **112**, 109662.

Cremades, Andrés, Hoyas, Sergio & Vinuesa, Ricardo 2025*b* Classically studied coherent structures only paint a partial picture of wall-bounded turbulence. *Nature Communications* **16** (1), 10189.

Erion, Gabriel, Janizek, Joseph D, Sturmfels, Pascal, Lundberg, Scott M & Lee, Su-In 2021 Improving performance of deep learning models with axiomatic attribution priors and expected gradients. *Nature machine intelligence* **3** (7), 620–631.

Guastoni, Luca, Güemes, Alejandro, Ianiro, Andrea, Discetti, Stefano, Schlatter, Philipp, Azizpour, Hossein & Vinuesa, Ricardo 2021 Convolutional-network models to predict wall-bounded turbulence from wall quantities. *Journal of Fluid Mechanics* **928**, A27.

Hoyas, Sergio, Benedikt, Nils, Cremades, Andres & Vinuesa, Ricardo 2025 Deep-learning-based assessment of skin friction in wall-bounded turbulence. *Physical Review Fluids* **10** (6), L062601.

Jiménez, Javier 2018 Coherent structures in wall-bounded turbulence. *Journal of Fluid Mechanics* **842**, P1.

Lundberg, Scott M & Lee, Su-In 2017 A unified approach to interpreting model predictions. *Advances in neural information processing systems* **30**.

Moody, Lewis F. 2022 Friction Factors for Pipe Flow. *Transactions of the American Society of Mechanical Engineers* **66** (8), 671–678.

Osawa, Kosuke & Jiménez, Javier 2024 Causal features in turbulent channel flow. *arXiv preprint arXiv:2405.15674* .

Pope, S. B. 2000 *Turbulent flows*. Cambridge: Cambridge University Press.

Ronneberger, Olaf, Fischer, Philipp & Brox, Thomas 2015 U-net: Convolutional networks for biomedical image segmentation. In *Medical Image Computing and Computer-Assisted Intervention–MICCAI 2015: 18th International Conference, Munich, Germany, October 5-9, 2015, Proceedings, Part III 18*, pp. 234–241. Springer.

Slotnick, J., Khodadoust, A., Alonso, J., Darmofal, D., Gropp, W., Lurie, E. & Mavriplis, D. 2014 CFD Vision 2030 Study: A Path to Revolutionary Computational Aerosciences. *NASA TECHNICAL REPORT* (218178).